

Supplementary Materials for

**METTL14 is a chromatin regulator independent of its RNA *N*<sup>6</sup>-methyladenosine methyltransferase activity**

Xiaoyang Dou<sup>1,2,11</sup>, Lulu Huang<sup>3,4,11</sup>, Yu Xiao<sup>1,2,11</sup>, Chang Liu<sup>1,2,5</sup>, Yini Li<sup>6</sup>, Xinning Zhang<sup>3,4</sup>,  
Lishan Yu<sup>3,4</sup>, Ran Zhao<sup>3,4</sup>, Lei Yang<sup>7</sup>, Chuan Chen<sup>7</sup>, Xianbin Yu<sup>1,2</sup>, Boyang Gao<sup>1,2</sup>, Meijie Qi<sup>8</sup>,  
Yawei Gao<sup>7</sup>, Bin Shen<sup>9</sup>, Shuying Sun<sup>6</sup>, Chuan He<sup>1,2,10,\*</sup>, Jun Liu<sup>3,4,\*</sup>

**This file includes:**

Figs. S1 to S7

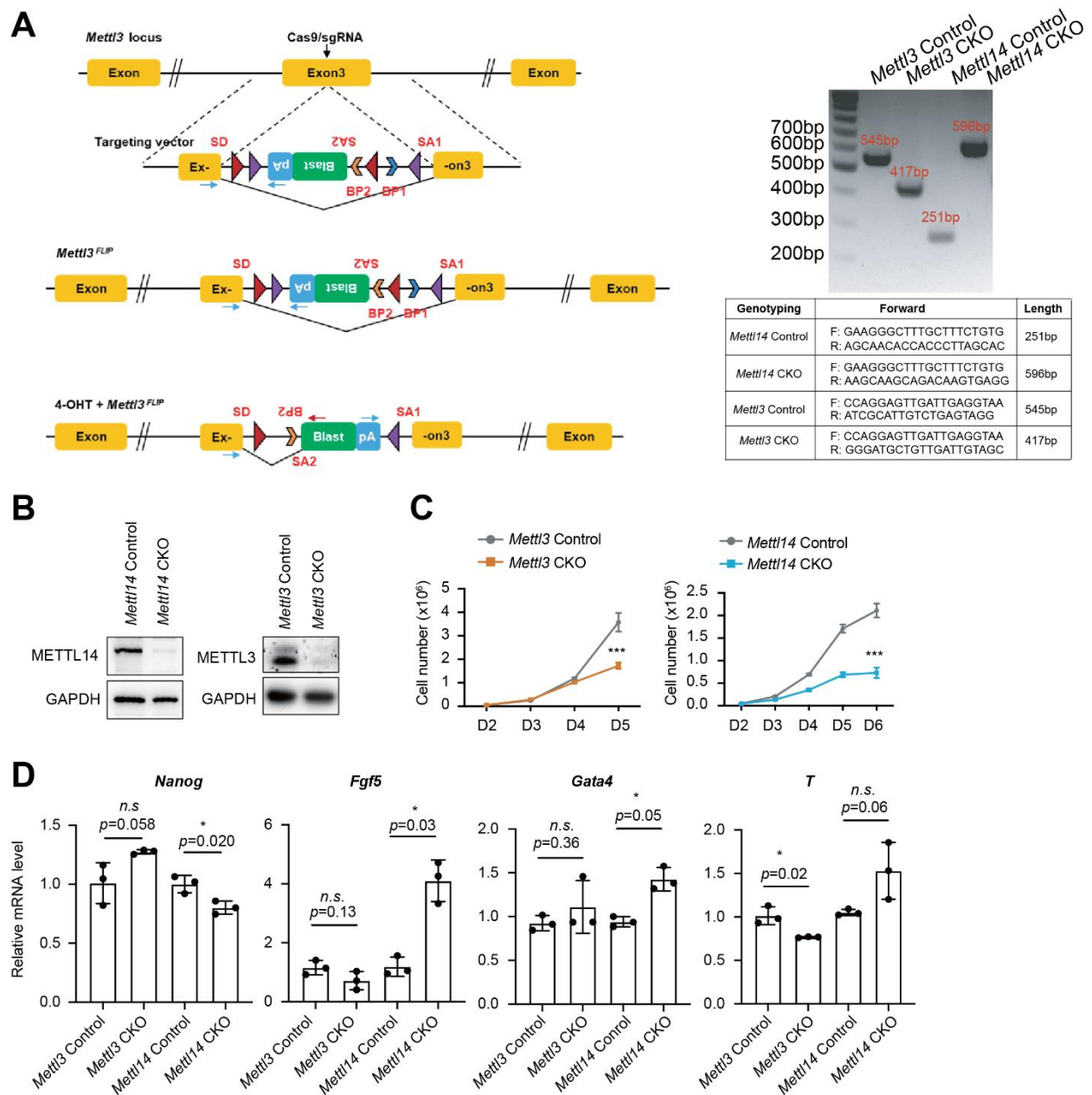


**Figure S1. METTL3 and METTL14 acted differently on stemness maintenance of mESCs.** (A) Construction and genotyping of *Mettl3* and *Mettl14* CKO mESCs. (B) Immunoblot assays of METTL14 protein levels in *Mettl14* Control and *Mettl14* CKO mESCs (left panel), and METTL3 protein levels in *Mettl3* Control and *Mettl3* CKO mESCs (right panel). (C) Cell proliferation assay of *Mettl3* Control, *Mettl3* CKO, *Mettl14* Control, and *Mettl14* CKO mESCs. n=3 per condition. \*\*\*P < 0.001. Two-tailed Student's t-test. (D) Bar plot of *Nanog*, *Fgf5*, *T* and *Gata4* expression in *Mettl3* Control, *Mettl3* CKO, *Mettl14* Control, and *Mettl14* CKO mESCs. \*P < 0.05. n = 3 biological replicates; Two-tailed Student's t-test.

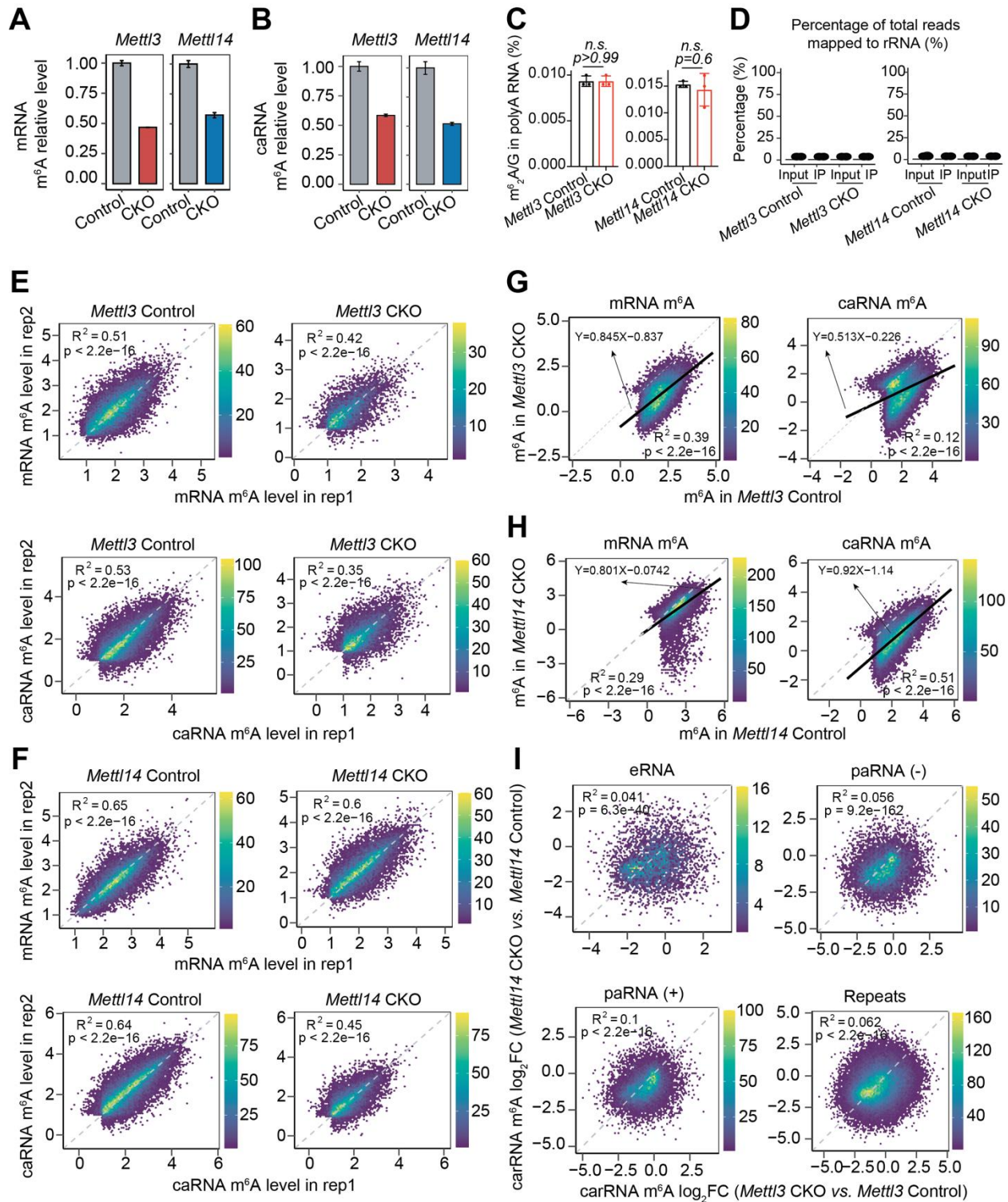


**Figure S2. METTL3 and METTL14 acted similarly on m<sup>6</sup>A-mediated regulation. (A-B)** m<sup>6</sup>A levels on mRNA (A) and caRNAs (B) in *Mettl3* Control and *Mettl3* CKO, *Mettl14* Control

and *Mettl14* CKO mESCs, respectively. m<sup>6</sup>A level were quantified using MeRIP-seq data with the number of reads mapped to mouse genome divided by the number of reads mapped to m<sup>6</sup>A modified spike-in. n = 2 biological replicates; error bars indicate means  $\pm$  SEM. **(C)** LC-MS/MS quantification of the m<sup>6</sup><sub>2</sub>A/G ratio of the PolyA-enriched RNA extracted from *Mettl3* Control, *Mettl3* CKO, *Mettl14* Control and *Mettl14* CKO mESCs. **(D)** The percentages of total reads mapped to rRNA in MeRIP-seq data of *Mettl3* Control, *Mettl3* CKO, *Mettl14* Control and *Mettl14* CKO mESCs. **(E-F)** The correlation of m<sup>6</sup>A level on mRNA (*top* two panels) and caRNA (*bottom* two panels) between two biological replicates in *Mettl3* Control and *Mettl3* CKO **(E)**, *Mettl14* Control and *Mettl14* CKO **(F)** mESCs, respectively. **(G-H)** The correlation of m<sup>6</sup>A level on mRNA (*left* panel) and caRNA (*right* panel) between *Mettl3* Control and *Mettl3* CKO **(G)**; and *Mettl14* Control and *Mettl14* CKO **(H)** in mESCs. **(I)** The correlation of m<sup>6</sup>A fold-changes (log<sub>2</sub>FC) on carRNAs including eRNA, sense paRNAs (paRNA(+)), antisense paRNAs (paRNA(-)) and repeats RNAs between *Mettl14* CKO *vs.* *Mettl14* Control and *Mettl3* CKO *vs.* *Mettl3* Control mESCs.

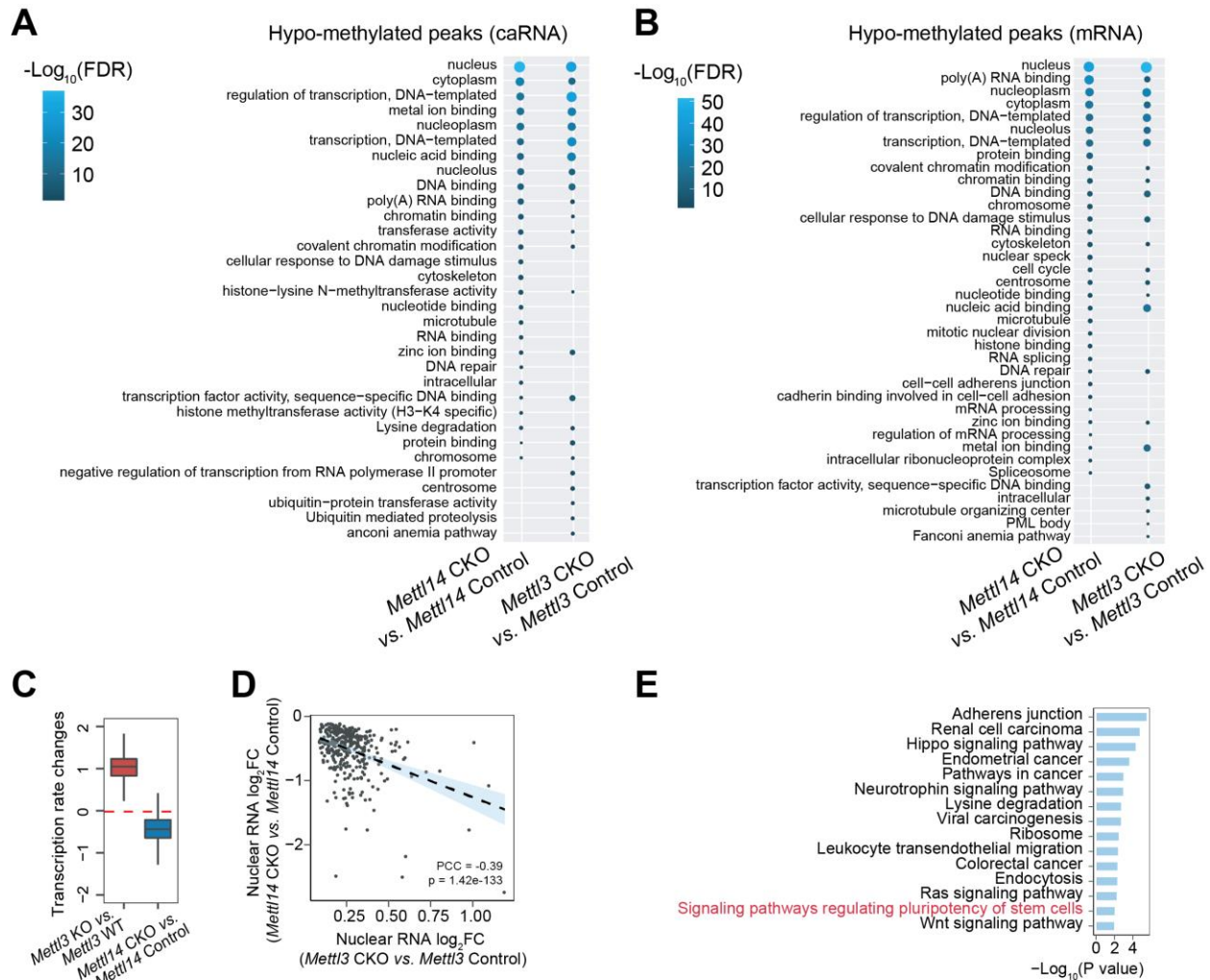


**Figure S3. METTL3 and METTL14 differed in transcriptome regulation.** (A-B) Enrichment analysis of genes harbored hypo-methylated peaks in caRNA (A) or mRNA (B) upon *Mettl3* knockout (A) or *Mettl14* knockout (B) in mESCs. (C) Boxplot of transcription rate changes upon *Mettl3* (GSE133582) or *Mettl14* knockout in mESCs. (D) The correlation of gene expression fold-changes ( $\log_2FC$ ) upon *Mettl3* or *Mettl14* knockout in mESCs. These genes are significantly (adjusted P [padj] < 0.05) up-regulated upon *Mettl3* knockout and down-regulated upon *Mettl14* knockout in mESCs. (E) KEGG pathway enrichment analysis of genes that are significantly (adjusted P [padj] < 0.05) up-regulated upon *Mettl3* knockout and down-regulated upon *Mettl14* knockout in mESCs.

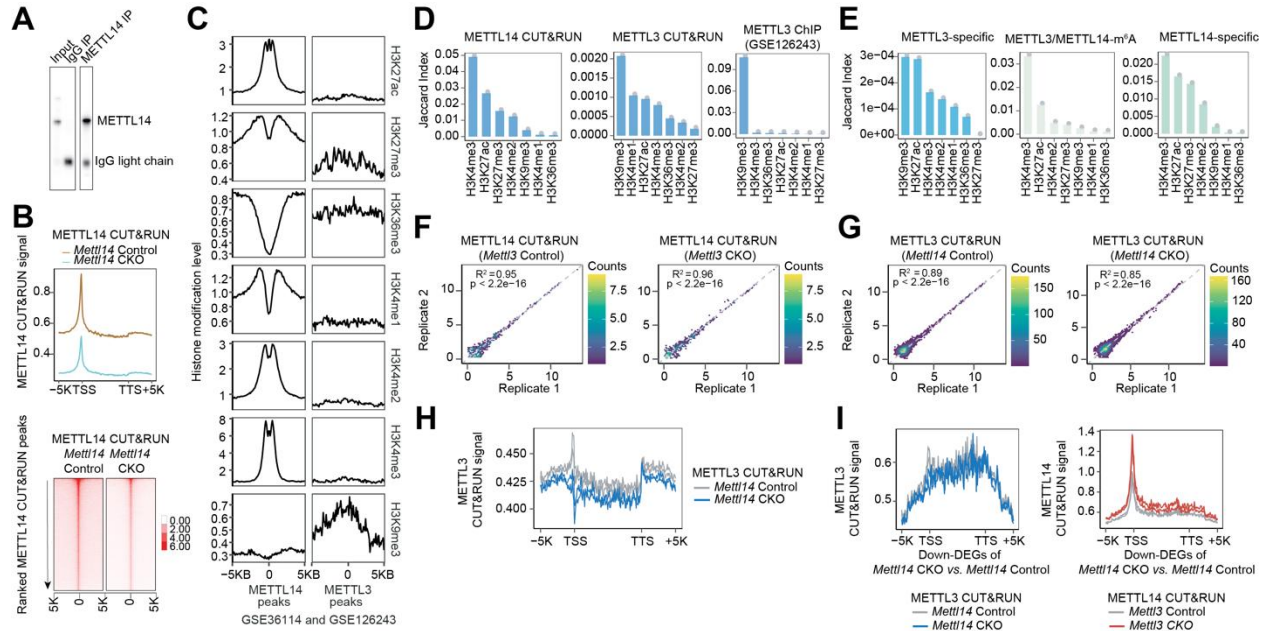


**Figure S4. METTL3 and METTL14 displayed distinct chromatin binding preferences.** (A) Western blot assays showing the specificity and IP efficiency of the METTL14 antibodies we used. (B) Average profiles of METTL14 at gene level (from 5KB upstream of TSS to 5KB downstream of TTS) in *Mettl14* Control or *Mettl14* CKO mESCs (top panel). Heatmap of METTL14 genomic binding at peaks center and their flanking regions in *Mettl14* Control or *Mettl14* CKO mESCs (bottom panel). CUT&RUN signal has been normalized to *E. coli* Spike-in DNAs. (C) Average profiles of various histone modification on METTL3 and METTL14 CUT&RUN peaks in wild type mESCs. (D) Bar graphs showing the overlapping ratios (Jaccard index) of METTL14 CUT&RUN, METTL3 CUT&RUN and METTL3 ChIP-seq peaks with different histone modifications (GSE36114 and GSE126243) in wild type mESCs. (E) Bar graphs showing the overlapping ratios (Jaccard index) of METTL14-specific sites, METTL3-specific sites and METTL3/METTL14-m<sup>6</sup>A sites with different histone modifications in wild type mESCs. (F-G) The correlations of METTL14 CUT&RUN signal between two biological replicates in *Mettl3* Control and *Mettl3* CKO mESCs (F), and METTL3 CUT&RUN signal between two biological replicates in *Mettl14* Control and *Mettl14* CKO mESCs (G). (H) Average profile of METTL3 CUT&RUN signal at gene level in *Mettl14* Control and *Mettl14* CKO mESCs. (I) Profiles of METTL14 and METTL3 CUT&RUN signals on genes that are significantly down-regulated (down-DEGs) upon *Mettl14* knockout in mESCs.

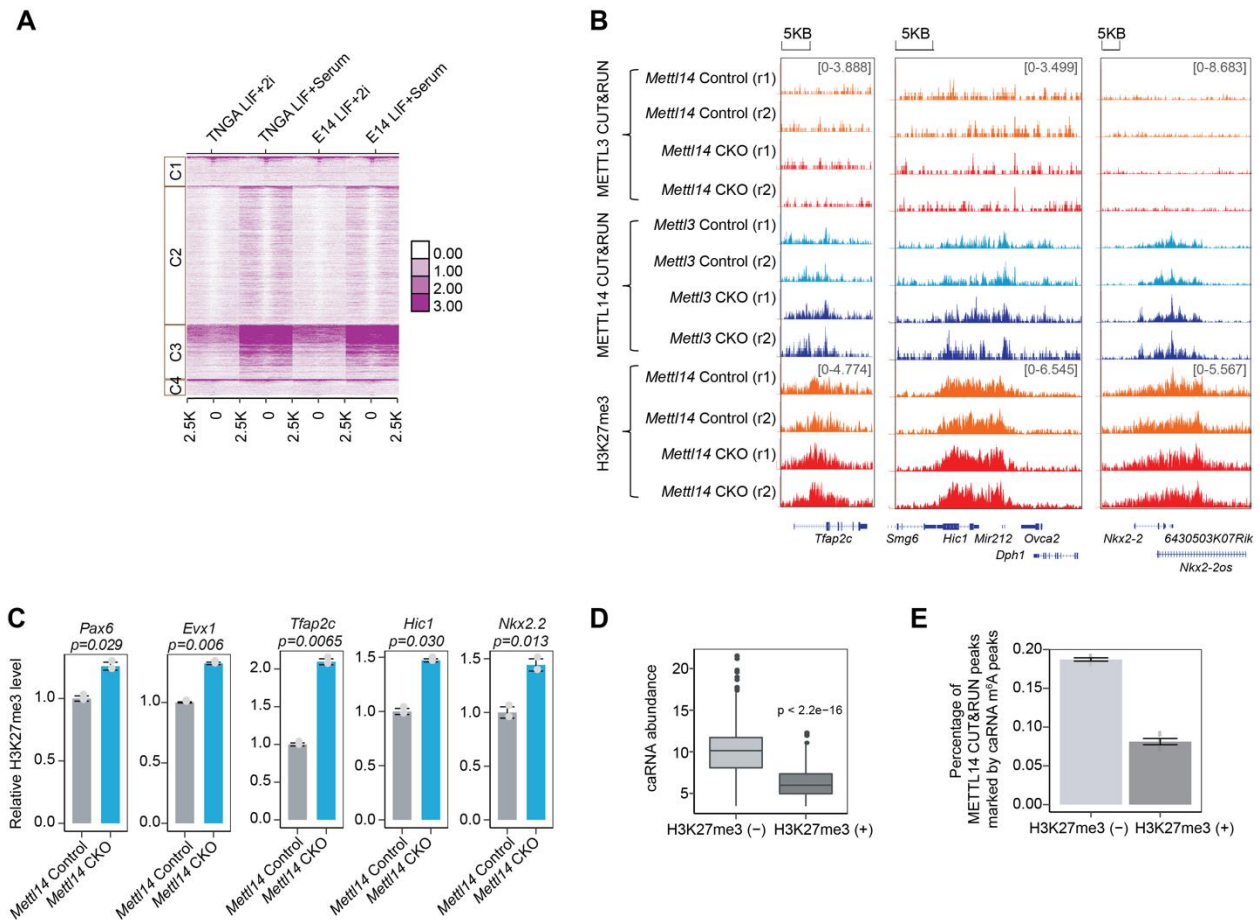


**Figure S5. METTL14-occupied genomic regions marked with H3K27me3 are less enriched of m<sup>6</sup>A than the non-marked ones.** (A) Heatmap of H3K27me3 modification at four identified clusters in mESCs cultured under different cell culture conditions: “LIF+Serum” condition refers to the presence of LIF in the medium containing Serum, and “LIF+2i” condition refers to serum-free medium containing 2i. (B-C) IGV visualization (B) and bar plot for quantification (C) showing H3K27me3 levels on *Tfp2c*, *Hic1* and *NKx2-2* genes in *Mettl14* Control and *Mettl14* CKO mESCs. (D) Boxplot of caRNA abundance that derived from METTL14 bound DNA loci. METTL14 peaks were categorized into H3K27me3 modified (H3K27me3 (+)) and unmodified (H3K27me3 (-)) groups. (E) Bar graph showing the percentage of METTL14 peaks overlapped with caRNA m<sup>6</sup>A peaks. METTL14 peaks were categorized into H3K27me3 modified (H3K27me3 (+)) and unmodified (H3K27me3 (-)) groups.

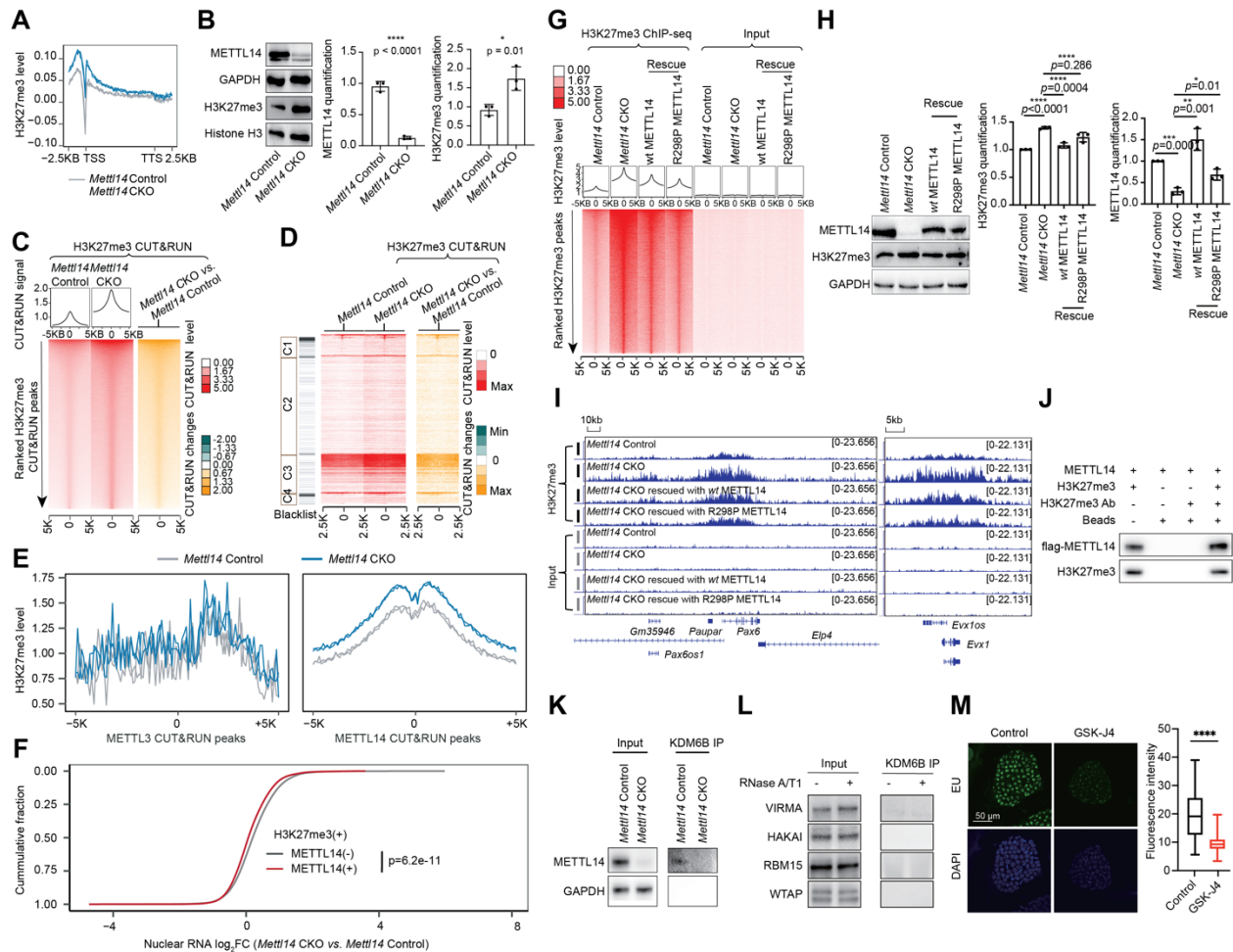


**Figure S6. METTL14 directly regulates H3K27me3 deposition in mESCs.** (A) Average profiles of H3K27me3 modification at gene level (from 2.5KB upstream of TSS to 2.5KB downstream of TTS) in *Mettl14* Control and *Mettl14* CKO mESCs, respectively. (B) Western blot (left panel) with quantification (right panel) of H3K27me3 in *Mettl14* Control and *Mettl14* CKO mESCs.  $n=3$  per condition. P values were calculated using Two-tailed Student's t-test. (C) Heatmap showing H3K27me3 CUT&RUN signal (left panel) and H3K27me3 signal changes (right panel) around the peak centers ( $\pm 5$ KB, left panel) upon *Mettl14* CKO in mESCs. CUT&RUN signal are normalized according to SNAP-CUTANA\_K-MetStat\_Panel\_Analysis pipeline. (D) Heatmap showing H3K27me3 binding and binding changes upon *Mettl14* knockout in mESCs at the four clusters of METTL3 and METTL14 peak centers and the flanking 2.5KB regions. (E) H3K27me3 modifications on METTL3 (left panel) or METTL14 (right panel) CUT& RUN peak centers and the flanking 5KB in *Mettl14* Control and *Mettl14* CKO mESCs, respectively. (F) Cumulative distributions of H3K27me3 modified gene expression fold-changes

(log<sub>2</sub>FC) upon *Mettl14* knockout in mESCs. H3K27me<sub>3</sub> modified genes were categorized into METTL14 bound (+) and unbound (-) groups. P values were calculated by a nonparametric Wilcoxon-Mann-Whitney test. (G) Heatmap showing H3K27me<sub>3</sub> ChIP-Rx signals around the peak centers (+/- 5KB) in *Mettl14* Control, *Mettl14* CKO, and *Mettl14* CKO mESCs rescued with wild-type METTL14 or R298P mutated METTL14. ChIP-seq signal has been normalized to *Drosophila* Spike-in DNAs. (H) Immunoblot assays (*left panel*) with quantification (*right panel*) of METTL14 and H3K27me<sub>3</sub> level in *Mettl14* Control, *Mettl14* CKO, *Mettl14* CKO rescued with wild-type METTL14 (*wt* METTL14) or with R298P mutated METTL14 (R298P METTL14) mESCs, respectively. (I) IGV profiles showing H3K27me<sub>3</sub> modification level and its inputs around *Pax6* and *Evx1* gene loci in *Mettl14* Control, *Mettl14* CKO, and *Mettl14* CKO mESCs rescued with wild-type METTL14 or R298P mutated METTL14, respectively. (J) Western blots of the *in vitro* immunoprecipitated H3K27me<sub>3</sub> peptide and its interaction with flag-METTL14. (K) Western blots of the immunoprecipitated KDM6B from *Mettl14* Control and *Mettl14* CKO mESCs and its interaction with METTL14. (L) Western blots of the immunoprecipitated KDM6B from mESCs and its interaction with the components of methyltransferase complex. (M) Analysis of nascent RNA synthesis in wild-type mESCs treated with DMSO and GSK-J4. Nascent RNA synthesis was detected by using a click-it RNA Alexa fluor 488 imaging kit. EU, 5-ethynyl uridine; DAPI, 4',6-diamidino-2-phenylindole.

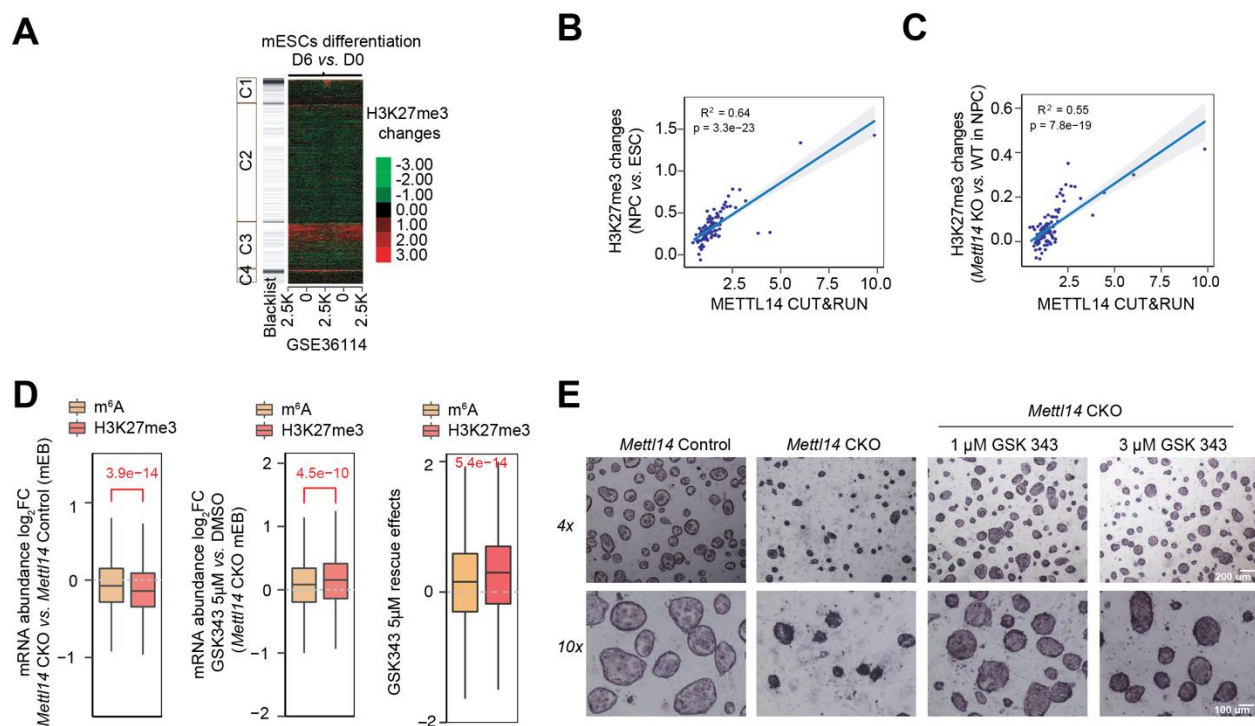


**Figure S7. METTL14 regulates H3K27me3 changes during neuronal differentiation of mESCs.** (A) Heatmap showing H3K27me3 modification level changes during mESCs differentiation (day 6 vs. day 0) on four clusters of METTL3 and METTL14 CUT&RUN peak centers and the flanking 2.5KB regions. (B-C) Scatter plot showing the correlation between METTL14 CUT&RUN signal and H3K27me3 level changes comparing NPCs vs. ESCs (B), and *Mettl14* KO vs. wildtype (WT) NPC (C). Sites ranked by METTL14 CUT&RUN signal were grouped and averaged into 100 data point. (D) Boxplot of gene expression level fold-changes ( $\log_2FC$ ) upon *Mettl14* knockout (left panel); after GSK343 treatment in *Mettl14* knockout mEB (middle panel); or the rescue degree (right panel). Rescue degree was calculated as  $\log_2FC$  from (middle panel) subtracted the  $\log_2FC$  from (left panel). Genes were categorized into two subgroups according to whether they were modified by m<sup>6</sup>A or H3K27me3. P values were calculated by a nonparametric Wilcoxon-Mann-Whitney test. (E) Alkaline phosphatase staining of *Mettl14* Control, *Mettl14* CKO, and *Mettl14* CKO mESCs treated with GSK343 under two different concentrations.